Ion-exchange bonded $H_2Ti_3O_7$ nanosheets-based magnetic nanocomposite for dye removal via adsorption and its regeneration via synergistic activation of persulfate

Manu Jose, P.T. Aswathi, K. Sriram, Priyadarshini Parakh,

Halan Prakash, Satyajit Shukla

†Electronic Supplementary Information (ESI)

(A)

A.1 Synthesis of HTNS

The spherical flyash (FA) particles (1-5 μM in size) were obtained from the National Thermal Power Corporation (NTPC), Ramagundam, India. The as-received FA particles were first surface-coated with anatase-titania (TiO_2) via sol-gel method. For this, 5 g of as-received FA particles were suspended under the continuous stirring, using an overhead stirrer (IKA Eurostar Digital, Germany), in 125 ml solution of 0.1 M (final concentration) titanium(IV) iso-propoxide ($Ti(OC_3H_7)_4$, 98 %, Sigma-Aldrich, India) dissolved completely in 2-propanol (>99.5 %, Sigma-Aldrich, India). To this suspension, a clear solution of distilled water dissolved in 125 ml of 2-propanol was added dropwise under the continuous stirring. The *R*-value of 5 (defined as the ratio of molar concentration of water to that of $Ti(OC_3H_7)_4$ precursor) was selected for obtaining TiO_2-coating on the surface of FA particles via hydrolysis and condensation of precursor. The TiO_2-coated FA particles were separated from the solution using a centrifuge (R23, Remi Instruments Ltd., Mumbai, India) and dried in an oven at 80^oC overnight. The amorphous-TiO_2 coated FA particles were then calcined in a furnace at 600^oC for 2 h at the heating rate of 3^oC min^{-1} to obtain the anatase-TiO_2 coated FA particles. With this procedure, the FA-anatase-TiO_2 composite particles containing ~30 wt% anatase-TiO_2 was obtained.

5 g of anatase-TiO_2 coated FA particles were treated under the hydrothermal condition in an autoclave (Amar Equipment Pvt. Ltd., Mumbai, India) at 120^oC for 30 h in a highly alkaline solution of 10 M sodium hydroxide (NaOH, 97%, S.D. Fine-Chem Ltd., India). The autoclave was allowed to cool naturally to room temperature and hydrothermal product was separated by

decanting the top solution. The product was washed using 100 ml of 1 M hydrochloric acid (HCl, Qualigens Fine Chemicals, India) solution for 1 h followed by washing with 100 ml of pure distilled water for 1 h. After centrifuging, the product was then subjected to another washing-cycle consisting washing with 100 ml of 1 M HCl for 1 h and then multiple times (#8-9) using 100 ml of pure distilled water for 1 h till pH (Hanna HI 2210 Bench Top, Sigma-Aldrich, India) of the filtrate became almost constant or neutral. The washed-product was then separated from the solution using a centrifuge and dried in an oven at 80^{o}C overnight to obtain HTNS.

A.2 Synthesis of HTNSF magnetic nanocomposites

The HTNSF magnetic nanocomposites having varying weight-fractions (5, 10, and 25 wt%) of γ-Fe_2O_3 nanoparticles (Aldrich Chemicals, Bengaluru, India) were synthesized via simple mechanical mixing involving an ion-exchange mechanism. In this method, an appropriate quantities of γ-Fe_2O_3 nanoparticles and HTNS were dispersed separately in equal quantities of two different aqueous solutions at neutral solution-pH (~6.5) using an ultrasonication bath (Bandelin Sonorex Super with Built-In Heating, Aldrich Labware, Bengaluru, India). The two suspensions were then mixed together to form total 1 g of solid particles suspended in 125 ml aqueous solution at neutral solution-pH which was stirred vigorously using an overhead stirrer (IKA RW 14, Aldrich Labware, Bengaluru, India) for 8 h at 600 rpm. The brownish product formed was separated using an external magnetic field provided by a small bar magnet and dried in an oven at 80^{o}C overnight to obtain HTNSF magnetic nanocomposites.

A.3 Characterization of HTNS and HTNSF magnetic nanocomposites

The morphology and average size of different samples were determined using the transmission electron microscope (TEM, Tecnai G^2, FEI, The Netherlands) operated at 300 kV. (Note: The samples were ultrasonically dispersed in 30 ml acetone for 20 min in which the carbon-coated Cu-grid (Ted Pella, Inc., U.S.A.) of 3 mm diameter was dipped for the TEM sample preparation). The nanocrystalline nature of samples and different phases present were confirmed via obtaining the selected-area electron diffraction (SAED) patterns. The crystalline phases present were also determined using the X-ray diffraction (XRD, PW1710 Phillips, The Netherlands). The broad-scan analysis was typically conducted within the 2θ range of 5^o-80^o using the Cu$K\alpha$ (λ_{Cu}=1.542 Å) X-radiation. The specific surface-area and pore-size distribution were measured using the Brunauer-Emmett-Teller (BET) surface-area measurement technique (Micrometrics Gemini 2375 Surface Area Analyzer, U.S.A.) via nitrogen (N_2) adsorption using the multi-point method after degassing the samples in flowing N_2 at 200°C for 2 h. The magnetic properties of different samples were measured using a vibrating sample magnetometer (VSM) attached to a Physical Property Measurement System (PPMS, Quantum Design, Dynacool, U.S.A.). The pristine samples were subjected to different magnetic field strengths (H) and the induced magnetization (M) was measured at 298 K. The external magnetic field was reversed on saturation and the hysteresis loop was traced. The zeta-potential measurements were performed using the electrophoretic light scattering in the pH range of 1-10 using a Zetasizer Nano Series-Zen 3600 (Malvern Instruments, U.K.). The band-gap energy (E_{BG}) measurements were conducted by obtaining the absorption spectra using the UV–visible spectrophotometer (UV-2401 PC,

Shimadzu, Japan), operated in the diffuse reflectance (DR) mode, for the wavelengths within the range of 200–800 nm.

A.4 Dye-adsorption measurements using HTNS and HTNSF magnetic nanocomposites

A 125 ml of aqueous suspension, with the initial solution-pH adjusted at ~10 using the ammonium hydroxide (NH_4OH) solution (25% NH_3, Qualigens Fine Chemicals Pvt. Ltd., Mumbai, India), was prepared at room temperature (30^{o}C) by dissolving 7.5-250 μM of methylene blue (MB) dye (96%, heterocyclic aromatic compound with the chemical formula $C_{16}H_{18}ClN_3S$ and molecular weight of 319.85 g mol^{-1}, S.D. Fine-Chem Ltd., Mumbai, India) and then dispersing 0.4 g l^{-1} of catalyst powder. The suspension was stirred in the dark and 4 ml sample suspension was separated after each 10 min time interval for total 60 min. The catalyst powder was separated using either a centrifuge or an external magnetic field provided by a small bar magnet. The filtrate was then utilized for obtaining the absorption spectra using the UV-visible absorption spectrophotometer (UV-2401 PC, Shimadzu, Japan). The normalized concentration of surface-adsorbed MB was calculated using the equation of form,

$$\%MB_{adsorbed} = \left(\frac{\boldsymbol{C_0} - C_t}{\boldsymbol{C_0}} \right)_{MB} \times 100 \quad \text{(S1)}$$

which is equivalent of form,

$$\%MB_{adsorbed} = \left(\frac{\boldsymbol{A_0} - A_t}{\boldsymbol{A_0}} \right)_{MB} \times 100 \quad \text{(S2)}$$

where, C_0 (mg l^{-1}) and C_t (mg l^{-1}) correspond to MB concentration at the start and after the contact time t (min) with the corresponding absorbance of A_0 and A_t.

A.5 Regeneration and reuse of HTNSF-5 magnetic nanocomposite in the dye-removal application

0.4 g l^{-1} of HTNSF-5 magnetic nanocomposite was added to 125 ml aqueous solution of MB dye having the initial concentration of 90 μM at the initial solution-pH of 10 under the ambient temperature (30^{o}C) condition. The dye-adsorption measurements were then conducted using procedure similar to the one described in the previous section. The HTNSF-5 sample with the surface-adsorbed MB dye, after separation from the aqueous solution using an external magnetic field provided by a small bar magnet and subsequent drying in an oven at 80^{o}C overnight, was utilized for the second-cycle of dye-adsorption measurement conducted under the similar test-conditions. Total three successive cycles of dye-adsorption measurements were conducted. The HTNSF-5 sample, with 107 mg g^{-1} of MB dye adsorbed on its surface, was utilized for the regeneration experiments. For this purpose, the former was added to 100 ml of 30 wt% H_2O_2 solution (S.D. Fine-Chem Ltd., Mumbai, India) at room temperature (30^{o}C) and stirred continuously using an overhead stirrer for 3 h. The powder was separated from the aqueous solution using an external magnetic field provided by a small bar magnet, and after drying in an oven at 80^{o}C overnight, it was recycled for the fourth-cycle of dye-adsorption. Similar experiments were repeated for the demonstration of regeneration and reuse of HTNF-5 magnetic nanocomposite using the potassium persulfate ($K_2S_2O_8$, 99%, S.D. Fine-Chem Ltd., Mumbai, India) solution. The concentration of $K_2S_2O_8$ solution used was changed to 0.1 M (~3 wt%).

The regeneration and reuse of HTNSF-5 magnetic nanocomposite using $K_2S_2O_8$ solution was also demonstrated at higher temperature (75^{o}C) where five consecutive cycles of adsorption

and reuse were conducted without and with the involvement of intermediate regeneration step. The experimental conditions used were, however, different than those used under the ambient temperature (30^{o}C) condition. In the present case, during the adsorption part of experiment, total volume of the solution, initial dye and catalyst concentrations were changed to 3 ml, 60 μM, and 1.2 g l^{-1} respectively. After the first cycle of MB adsorption conducted for the contact time of 1 h, a bar magnet was placed outside the container to attract the magnetic nanocomposite on its walls and the treated solution was decanted. The bar magnet was removed and fresh 10 ml distilled H_2O was poured into the container to collect the magnetic nanocomposite sticking on the walls of container. The aqueous suspension of magnetic nanocomposite was then dried in an oven at 80^{o}C overnight and dried sample was utilized for the second-cycle of dye-adsorption measurement conducted under the similar test-conditions. Total five successive cycles of dye-adsorption measurements were conducted without the use of any intermediate regeneration step. Later, dye-adsorption experiments were repeated with the involvement of regeneration step which was conducted after the end of each cycle of dye-adsorption. In this case, dried HTNSF-5 magnetic nanocomposite with MB dye adsorbed on its surface was dispersed in 3 ml of 2 mM (0.06 wt%) $K_2S_2O_8$ solution (obtained via dilution method) maintained at 75^{o}C and stirred using an overhead stirrer (IKA, Eurostar Digital, Germany) for 1 h. The regenerated catalyst was separated from the aqueous solution using an external magnetic field provided by a small bar magnet; and after drying in an oven at 80^{o}C overnight, it was reused for the next-cycle of dye-adsorption. Total five successive cycles of adsorption were conducted with the involvement of intermediate regeneration step.

A.6 Trapping of free hydroxyl radicals (•OH)

125 ml aqueous solution (or suspension) was prepared by completely dissolving 5×10^{-4} M of terephthalic acid (TA, 98%, Sigma-Aldrich Chemicals, Bangalore, India) and 2×10^{-3} M of sodium hydroxide (NaOH, Assay 97%, S.D. Fine-Chem Ltd., Mumbai, India) without and with suspending 0.4 g l^{-1} of HTNSF-5 magnetic nanocomposite. This was followed by the addition of 0.1 M (~3 wt%) of $K_2S_2O_8$ under continuous overhead stirring at room temperature (30^{o}C) and 4 ml sample suspension was separated after each 20 min time interval for total 60 min. The catalyst powder was separated using a bar magnet and the filtrate was then utilized for obtaining the photoluminescence (PL) (Cary Eclipse, Varian, The Netherlands) spectra. The trapping of free •OH by TA results in the formation of 2-hydroxyterephthalic acid which exhibits a characteristic PL peak located at ~425 nm at an excitation wavelength of ~315 nm. The intensity of PL peak is regarded as a measure of the amount of free •OH, and hence, that of the sulfate radical ions ($SO_4^{\bullet-}$) produced at a given time due to the activation of $S_2O_8^{2-}$. The intensity of PL peak from the solution, obtained without the addition of $K_2S_2O_8$, is regarded as a reference peak (that is, time t=0 min).

(B)

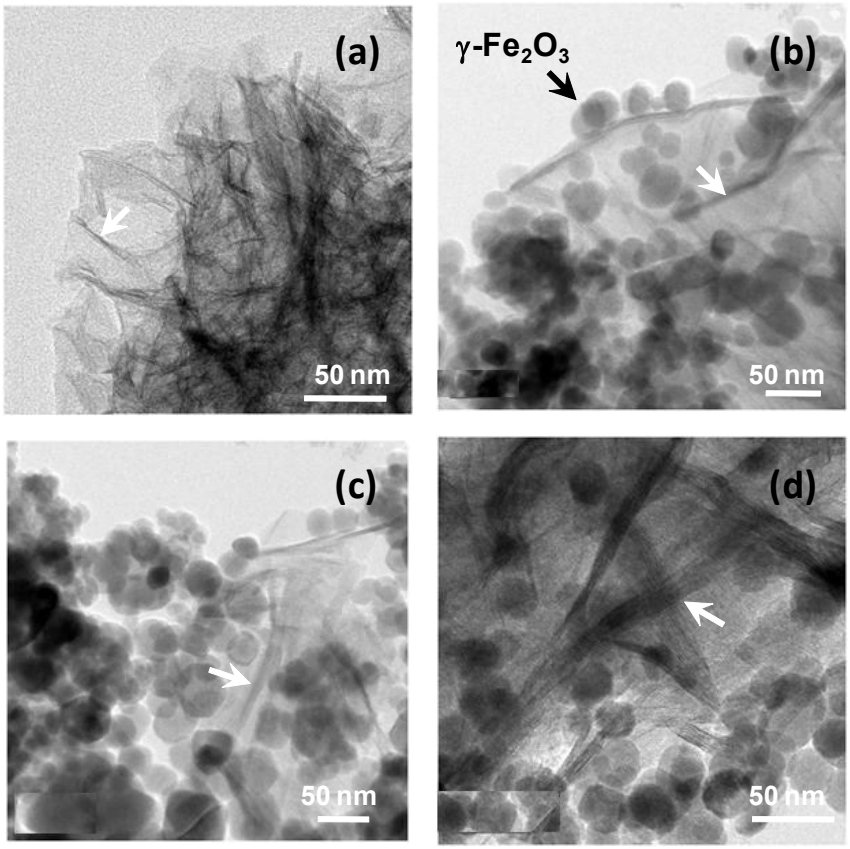

Fig. S1 High magnification TEM images of HTNS (a), HTNSF-5 (b), HTNSF-10 (c), and HTNSF-25 (d) magnetic nanocomposites. The white arrows indicate the thickness of stacked nanosheets within the aggregates.

(C)

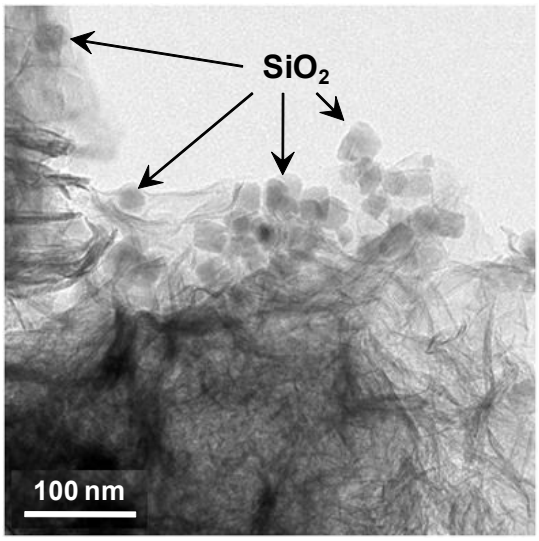

Fig. S2 TEM image showing attachment of SiO_2 nanoparticles at the edges of HTNS.

(D)

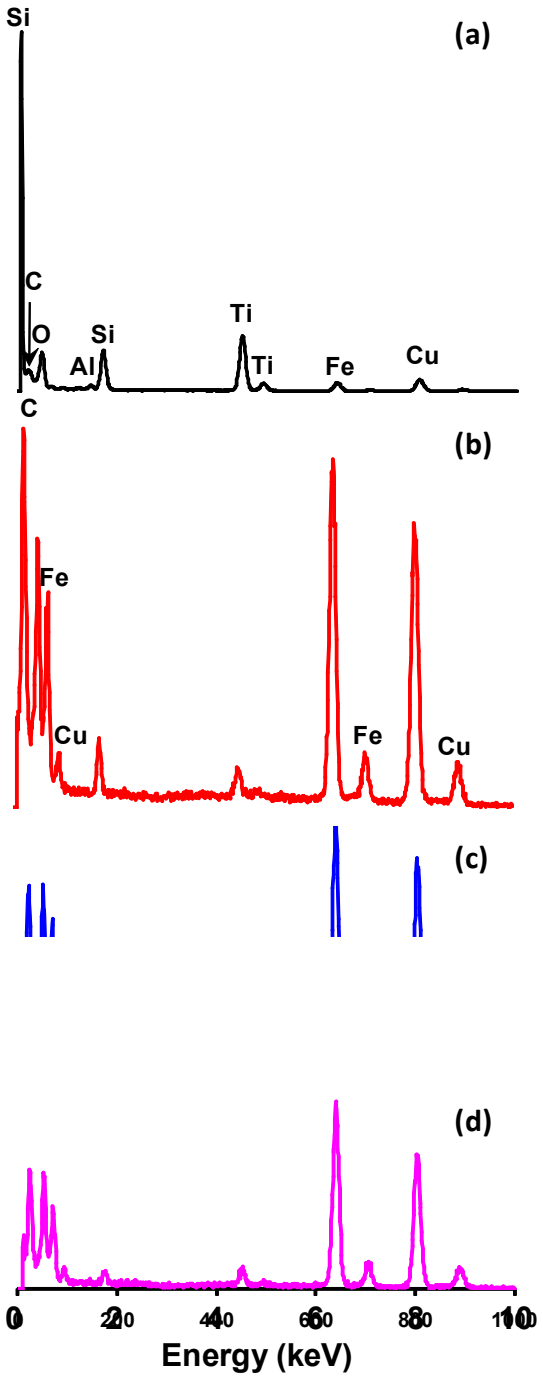

Fig. S3 EDX analyses of HTNS (a), HTNSF-5 (b), HTNSF-10 (c), and HTNSF-25 (d) magnetic nanocomposites. The Cu peak originates from the grid used for TEM analysis.

(E)

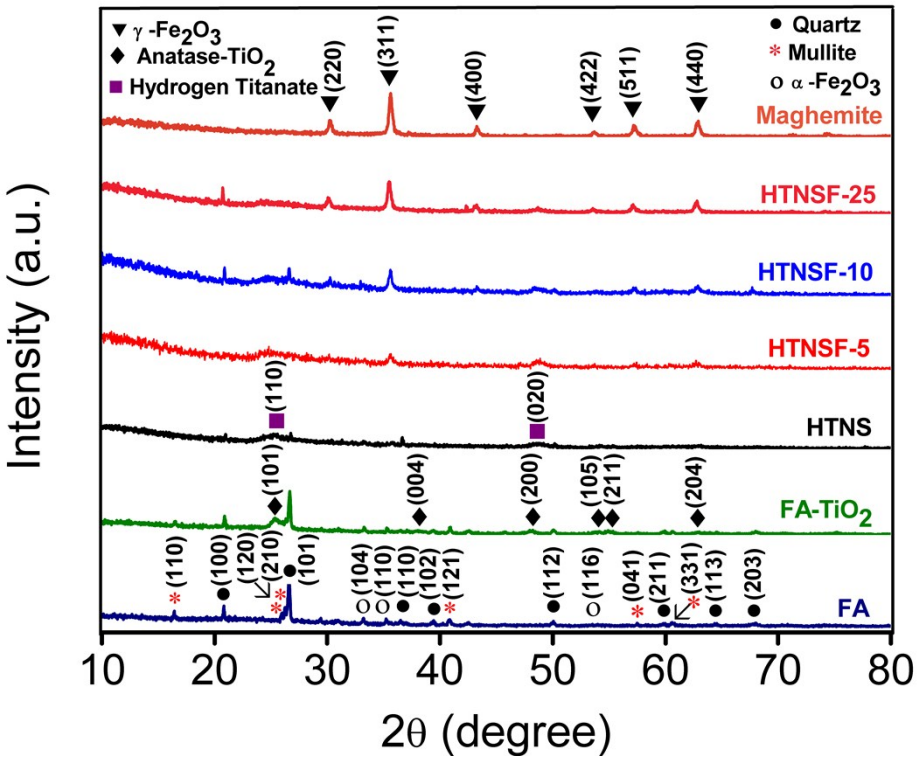

Fig. S4 XRD patterns as obtained for different samples.

(F)

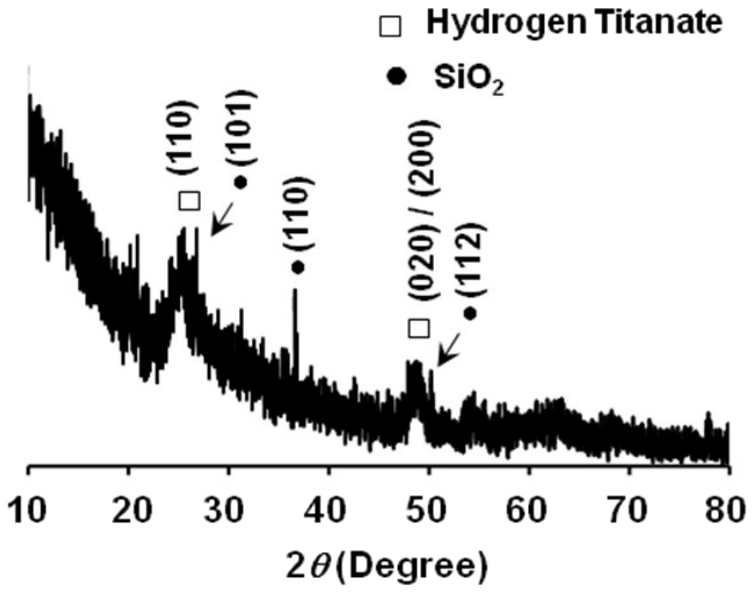

Fig. S5 Enlarged view of XRD pattern of HTNS showing the presence of SiO_2 phase along with that of hydrogen titanate phase.

(G)

Table S1. Identified phases, diffraction angles, and corresponding JCPDS card numbers (or the reference numbers) for the diffraction patterns presented in Figs. S4 and S5.

Identified Phase	Diffraction Angle 2θ (Degree) (Diffracting Plane)	JCPDS Card No. / [Reference]
SiO_2 (Quartz)	20.81 (100)	46-1015
	26.59 (101)	
	36.52 (110)	
	39.43 (102)	
	50.06 (112)	
	59.97 (211)	
	63.99 (113)	
	68.04 (203)	
$Al_6Si_2O_{13}$ (Mullite)	16.42 (110)	15-0776
	25.95 (120)	
	26.24 (210)	
	40.89 (121)	
	57.56 (041)	
	60.74 (331)	
α-Fe_2O_3 (Hematite)	33.16 (104)	33-0664
	35.21 (110)	
	53.97 (116)	
Anatase-TiO_2	25.36 (101)	21-1272
	37.85 (004)	
	48.19 (200)	
	54.09 (105)	
	55.16 (211)	
	62.83 (204)	
Hydrogen Titanate ($H_2Ti_3O_7$)	25.41 (110)	[19,20]
	48.52 (020) / (200)	
γ-Fe_2O_3 (Maghemite)	30.24 (220)	39-1346
	35.62 (311)	
	43.26 (400)	
	53.67 (422)	
	57.16 (511)	
	62.91 (440)	

(H)

It has been demonstrated that if the hydrothermal treatment is carried out by using pure anatase-TiO_2 precursor then nanosheets immediately roll to form nanotubes $H_2Ti_3O_7$ rather than the other types of structures with interlayer spacing of 0.78 nm within the walls of nanotubes.[15,21] Since, in the present investigation, the intermediate nanosheet morphology is stabilized by using the flyash-TiO_2 as precursor, it is assumed here that the structure of HTNS resembles that of $H_2Ti_3O_7$. According to the formation mechanism of nanosheets of $H_2Ti_3O_7$ as proposed by Hareesh et al.,[10] in highly alkaline aqueous solution under the hydrothermal conditions, anatase-TiO_2 coating on the surface of flyash tends to form large blocks of sodium titanate ($Na_2Ti_3O_7$); while, the flyash particles become disintegrated and get dissolved in the surrounding alkaline medium. Large amount of silicate ions (SiO_4^{4-}) and SiO_2 nanoparticles are released in this process from the flyash which may remain intercalated within and adsorbed on the surface of blocks of $Na_2Ti_3O_7$. During the subsequent washing in HCl solution and pure H_2O, an exfoliation of single nanosheets take place simultaneous with the operation of ion-exchange mechanism in which Na^+ ions are replaced with protons (H^+) forming $H_2Ti_3O_7$ phase. Due to the presence of large amount of surface-adsorbed SiO_4^- ions, Fig. S3a, and SiO_2 nanoparticles attached to the edges of the nanosheets, Fig. S2, the rolling of latter to nanotube morphology is strongly prevented due to reduction in the number of dangling bonds on the surface of nanosheets. In the support of this mechanism, the presence of SiO_2 nanoparticles is also detected in the XRD patterns of HTNS presented in Figs. S4 and S5.

(I)

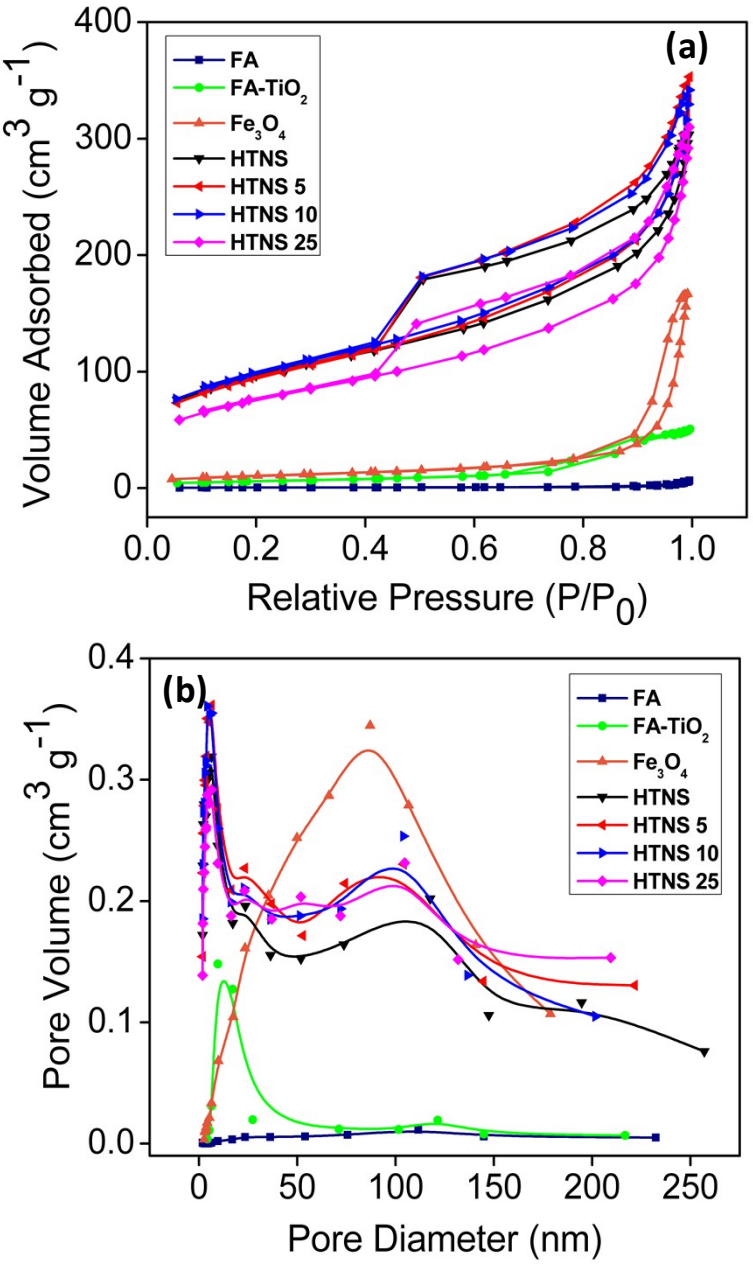

Fig. S6 N_2 adsorption / desorption isotherm curves (a) and the corresponding BJH pore-size distribution curves (b) as obtained for different samples.

As seen in Fig. S6b, all the samples except as-received γ-Fe_2O_3 nanoparticles, show bimodal pore-size distribution and presence of large amount of mesopores within the structure in accordance with the BET analysis which appears to be the prominent features of HTNS and HTNSF magnetic nanocomposites. The peaks at the average pore size of 4.5-6 nm and 100 nm are possibly due to the intra- and inter-aggregate porosities in agreement with the TEM analysis.

(J)

Table S2. Values of specific surface-area and pore volume as obtained for different samples.

Sample	Specific Surface-Area (m^2 g^{-1})	Pore Volume (cm^3 g^{-1})
Flyash	2.0	0.0086
Flyash-TiO_2	21.5	0.08
HTNS	334	0.45
HTNSF-5	334	0.51
HTNSF-10	346	0.495
HTNSF-25	269	0.448
γ-Fe_2O_3	37	0.263

It is to be noted that $H_2Ti_3O_7$ has a monoclinic crystal structure having the lattice parameters as provided in the Table S3.

Table S3. Lattice parameters of $H_2Ti_3O_7$.[S1,S2]

Material	a (Å)	b (Å)	c (Å)
$H_2Ti_3O_7$	16.0243	3.74973	9.1888

S1 A. Eguia-Barrio, E. Castillo-Martinez, M. Zarrabeitia, M. A. Munoz-Marquez, M. Casas-Cabanas and T. Roj, *Phys. Chem. Chem. Phys.* 2015, **17**, 6988.

S2 K. Kataoka, N. Kijima and J. Akimoto, *Inorg. Chem.* 2013, **52**, 13861.

To calculate the theoretical specific surface-area (SSA), we assume the $H_2Ti_3O_7$ nanosheet with one unit cell thickness of 0.91888 nm as a single layer. Hence, the specific surface-area of $H_2Ti_3O_7$ nanosheets with *N* layers can be calculated as,

$$SSA = \frac{2ab}{(NZM)/N_{AV}} \tag{S3}$$

where, *Z* represents the number of formula units per unit cell, *M* the molecular weight of $H_2Ti_3O_7$ (257.6127 g mol^{-1}), and N_{AV} the Avogadro's number (6.023×10^{23} mol^{-1}).

Substituting appropriate values in the eqn (S3), we get

$$SSA = \frac{2810}{NZ} \tag{S4}$$

Hence, for $H_2Ti_3O_7$ nanosheet with a single layer (N=1), we get

For Z=1, SSA = 2810 m^2 g^{-1}

For Z=2, SSA = 1405 m^2 g^{-1}

For Z=3, SSA = 937 m^2 g^{-1}

For Z=4, SSA = 703 m^2 g^{-1}, and so on.

Since the actual specific surface-area is measured to be 334 m^2 g^{-1}, the aforementioned theoretical calculations suggest that the $H_2Ti_3O_7$ nanosheets are made up of number of stacking layers (N>1) and are highly aggregated in agreement with the TEM analysis.

(K)

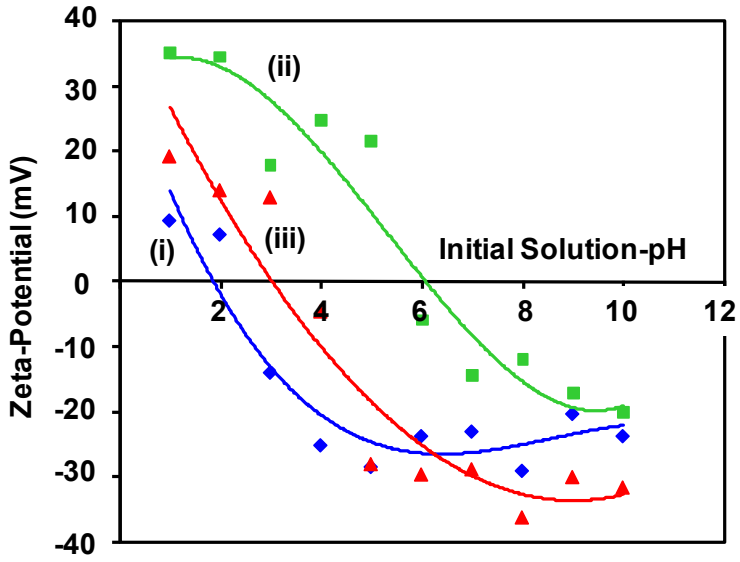

Fig. S7 Variation in the zeta-potential of HTNS (i), γ-Fe_2O_3 nanoparticles (ii), and HTNSF-5 magnetic nanocomposite (iii) as a function of initial solution-pH. The point-of-zero charge is determined to be at the initial solution-pH of 2.0, 6.0, and 3.0 respectively.

(L)

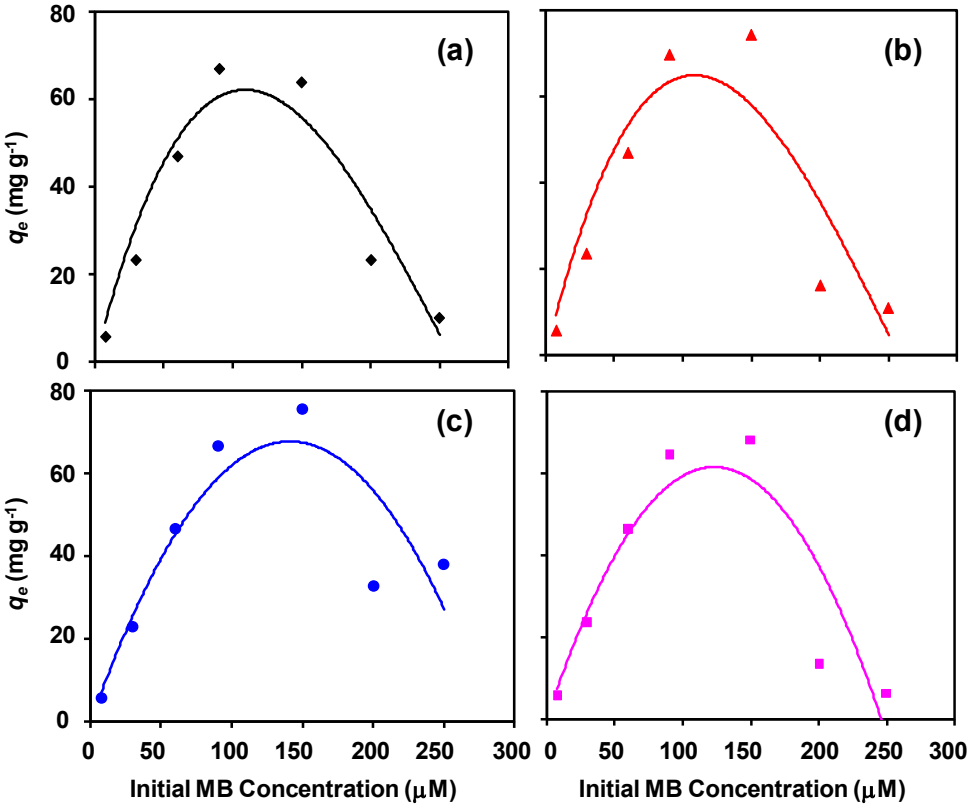

Fig. S8 Variation in q_e as a function of initial MB concentration as determined at the initial solution-pH value of 10 for different catalyst samples – HTNS (a), HTNSF-5 (b), HTNSF-10 (c), and HTNSF-25 (d).

(M)

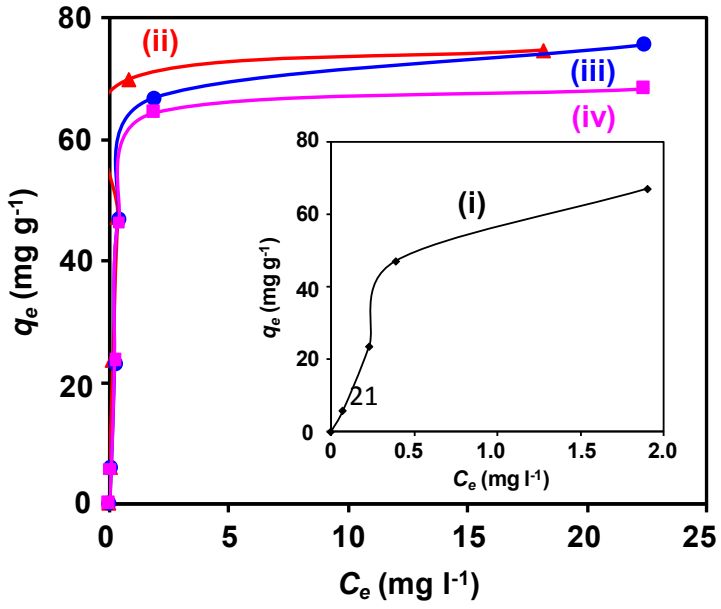

Fig. S9 Equilibrium adsorption isotherms for MB on different catalyst samples – HTNS (see the inset) (i), HTNSF-5 (ii), HTNSF-10 (iii), and HTNSF-25. (Note: data points above the peak values, Fig. S7, are not considered).

(N)

The linear forms of Lagergren pseudo-first-order and pseudo-second-order kinetics models can be respectively expressed as,

$$\log(q_e - q_t) = \log(q_e) - \left(\frac{k_1}{2.303}\right)t \quad \text{(S5)}$$

$$\frac{t}{q_t} = \left(\frac{1}{q_e}\right)t + \frac{1}{q_e^2 k_2} \quad \text{(S6)}$$

where, k_1 (min^{-1}), and k_2 (g mg^{-1} min^{-1}) are Lagergren pseudo-first-order rate-constant, pseudo-second-order rate-constant, and q_t the amount of MB adsorbed on the surface per unit mass (mg g^{-1}) of catalyst after the contact of time of t. (Note: in the present investigation, the intraparticle diffusion model[S3] is found to be invalid based on the lower values of regression correlation coefficient ($<r^2>$). Hence, it is not presented here).

S3 B. K. Babu, J. V. Purayil, H. Padinhattatyil, S. Shukla and K. G. Warrier, *Int. J. Appl. Ceram. Technol.* 2013, **10**, 186.

(O)

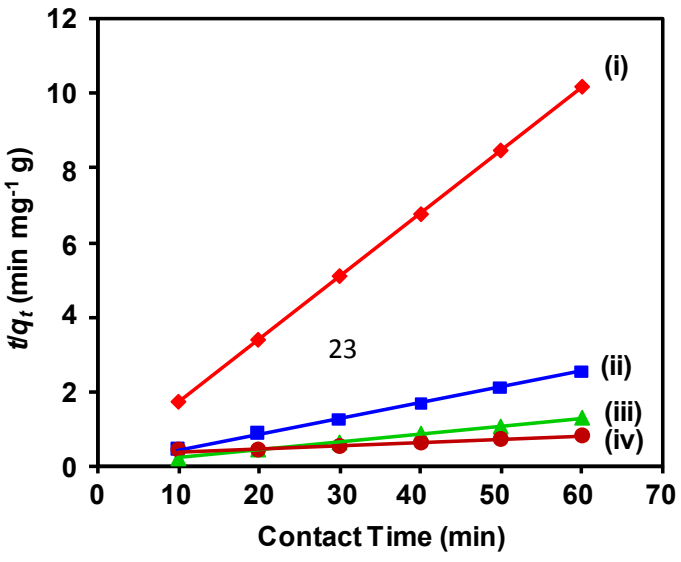

Fig. S10 Typical pseudo-second-order kinetics plots as obtained for the HTNSF-5 sample for different initial MB concentrations – 7.5 (i), 30 (ii), 60 (iii), and 150 μM (iv).

(P)

The equilibrium adsorption of MB on the surface of HTNS and HTNSF magnetic nanocomposites is analyzed using three well known adsorption isotherm models - Langmuir, Freundlich, and DKR. The Langmuir adsorption model is based on the assumption that all adsorption sites have equal affinity for adsorbate and permit monolayer adsorption. The concept of Freundlich model involves heterogeneity in the adsorption sites which allows the multilayer coverage. The type of interaction, whether ion-exchange or electrostatic attraction that exists in between the adsorbent and adsorbate, can be identified using the DKR model. The linear equation for above three models are as given below.

$$\frac{C_e}{q_e} = \left(\frac{1}{q_m}\right) C_e + \frac{1}{q_m K_L} \tag{S7}$$

$$\ln q_e = \left(\frac{1}{n}\right) \ln C_e + \ln K_F \tag{S8}$$

$$\ln q_e = \ln q_m - \beta\varepsilon^2 \tag{S9}$$

where, K_L (l mg^{-1}) is a Langmuir constant related to the Gibb's free-energy of adsorption, K_F (mg$^{1-1/n}$ g^{-1} l$^{1/n}$) and n the Freundlich constants related to q_m and adsorption intensity, β (mol^2 J^{-2}) a constant related to adsorption energy, and ε (J mol^{-1}) the Polanyi potential which is given by,

$$\varepsilon = RT \ln(1 + \frac{1}{C_e}) \tag{S10}$$

where, R (J mol^{-1} K^{-1}) is a gas constant and T (K) the absolute temperature. The adsorption energy, E (kJ mol^{-1}), can be calculated using the relationship of form,

$$E = \frac{1}{\sqrt{2\beta}} \times 10^{-3} \quad \text{(S11)}$$

When the E value is in between 8-16 kJ mol^{-1}, adsorption is due to the ion-exchange reactions; while, that less than 8 kJ mol^{-1} supports the electrostatic attraction mechanism.

Moreover, the degree of suitability of HTNS and HTNSF magnetic nanocomposites towards the adsorption of MB is estimated from the values of separation factor (R_L), which can be calculated from the following equation,

$$R_L = \frac{1}{1 + K_L C_o} \quad \text{(S12)}$$

The adsorption process is unfavorable if R_L>1, linear if R_L=1, favorable if 0<R_L<1, or irreversible if R_L=0. Further, the spontaneity of MB adsorption on the surface of HTNS and HTNSF magnetic nanocomposites can be tested from the value of change in the Gibb's free energy (ΔG^0, J mol^{-1}) which is calculated using the equation,

$$\Delta G^0 = -RT \ln K_L \quad \text{(S13)}$$

(Q)

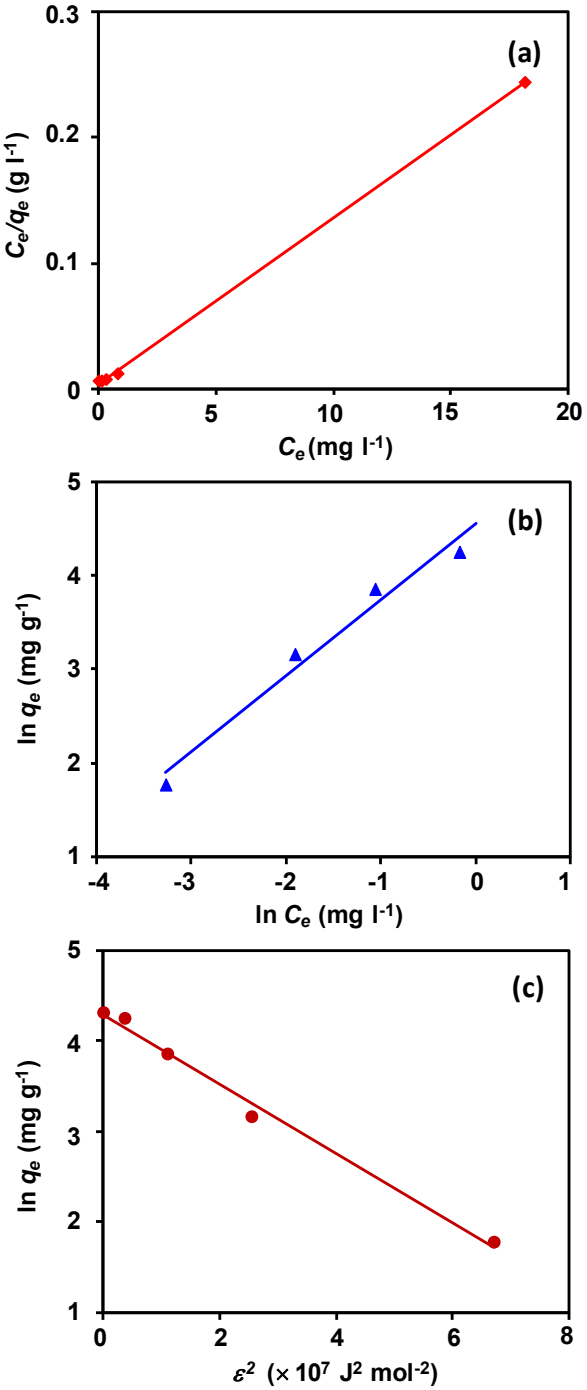

Fig. S11 Langmuir (a), Freundlich (b), and DKR (c) plots as obtained for HTNSF-5 magnetic nanocomposite.

(R)

It is to be noted that the unit of Y-axis scale in Fig. 11c is usually mol g^{-1}. However, in Fig. 11c, the Y-axis scale unit is converted to mg g^{-1} as per the following modification of eqn (S9).

$$Mq_e = Mq_m exp(-\beta\varepsilon^2) \quad \text{(S14)}$$

where, M is the molecular weight (mg mol^{-1}) of dye.

The eqn (S14) can be further modified as,

$$ln(Mq_e) = ln(Mq_m) - \beta\varepsilon^2 \quad \text{(S15)}$$

Hence, the graph of $ln(Mq_e)$ (mg g^{-1}) vs. ε^2 (J mol^{-1}) provides the same value of β as that is obtained using the eqn (S9). Moreover, Y-intercept provides the value of adsorption capacity directly with the units of mg g^{-1} instead of mol g^{-1}.

(S)

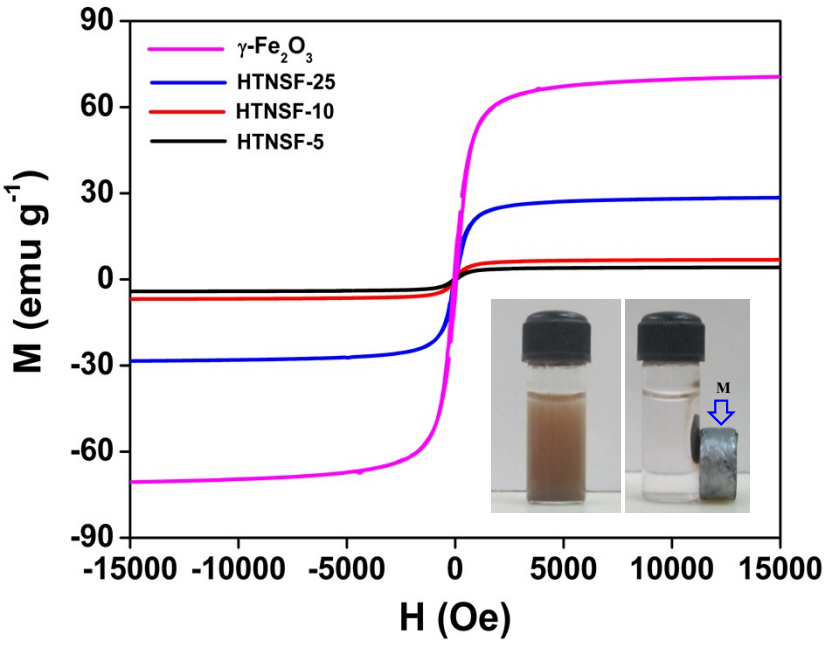

Fig. S12 Magnetization curves as obtained for different samples. The inset shows magnetic separation of HTNSF-5 nanocomposite from an aqueous solution. M represents an external magnet.

(T)

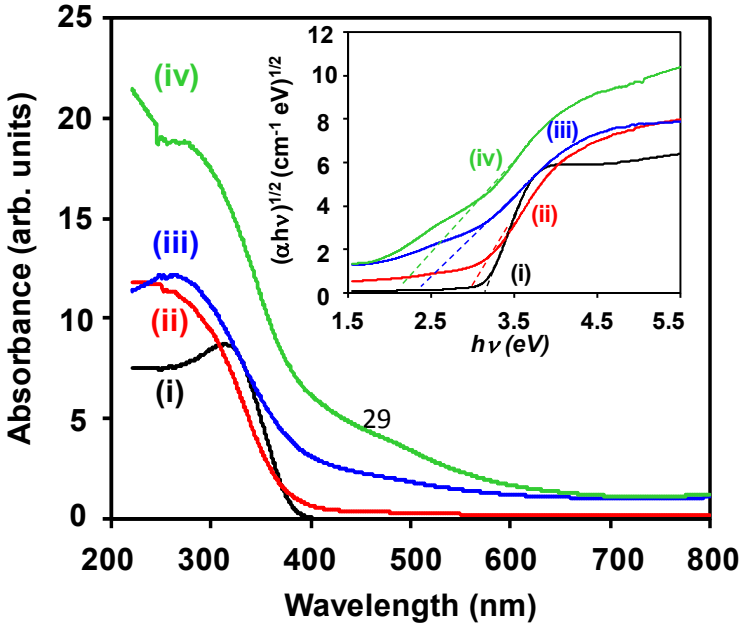

Fig. S13 UV-visible diffuse reflectance spectra obtained using different catalyst samples – anatase-TiO_2 (i), HTNS (ii), HTNSF-5 (iii), and HTNSF-10 (iv). The inset shows the corresponding plots of transformed Kubelka−Munk function versus energy of absorbed light.

The E_{BG} measurements show that anatase-TiO_2, HTNS, HTNSF-5, HTNSF-10, and γ-Fe_2O_3 nanoparticles (latter is not included in Fig. S12 for clarity) possess the E_{BG} values of 3.2, 2.9, 2.4, 2.1, and 1.97 eV respectively. Hence, it is clear that HTNS and HTNSF magnetic nanocomposites can easily absorb visible-light in solar-radiation under the normal ambient condition below the wavelength of 428 nm and 515-590 nm respectively which can generate the electron-hole pairs in the conduction and valance bands of HTNS. The visible-light induced electrons can then undergo photo-Fenton reaction generating $^{\bullet}OH$.[45]

$$H_2O_2 + e^- \rightarrow {}^{\bullet}OH + OH^- \quad \text{(S16)}$$

It, however, appears that the photo-Fenton reaction is hampered by lower amount of visible-light absorption by HNTS, poor adsorption of H_2O_2 their surfaces, and lack of effective interfacial charge transfer reaction which is attributed to the prior presence of SiO_4^{4-} ions and SiO_2 nanoparticles on their surfaces and edges. In addition to this, the photo-Fenton reaction, eqn (S16), is also possible to occur via generation of visible-light induced electron-hole pairs within the γ-Fe_2O_3 nanoparticles since it can absorb visible-light below the wavelength of 629 nm.[46] However, their weight-fraction in HTNSF-5 magnetic nanocomposite is very low to cause any significant activation of H_2O_2. The direct photolysis of H_2O_2 using UV-radiations having wavelengths in the range of 200-280 nm is reported to generate $^{\bullet}OH$ in large amount.[47] However, such an intense UV-light is not present in solar-radiation under the normal ambient conditions. Hence, the possibility of direct photolysis of H_2O_2 to generate $^{\bullet}OH$ in large amount is also ruled out.

Overall, as a consequence of various factors discussed above, H_2O_2 is not successfully activated by HTNSF-5 magnetic nanocomposite to generate $^{\bullet}OH$ during the regeneration treatment. Hence, the successful regeneration and reuse of HTNSF-5 magnetic nanocomposite could not be achieved using H_2O_2 activation technique; although, such technique is successfully utilized in the case of delaminated two-dimensional titanate nanosheets[12] and magnetic nanocomposites based on $H_2Ti_3O_7$ nanotubes[15] due to the absence of foreign species such as SiO_4^{4-} ions and SiO_2 nanoparticles on their surfaces and at the edges.